molecular pharmaceutics

ARTICLE

pubs.acs.org/molecularpharmaceutics

Critical Role of Organic Anion Transporters 1 and 3 in Kidney Accumulation and Toxicity of Aristolochic Acid I

Xiang Xue,[†,‡] Li-Kun Gong,[†,‡] Kazuya Maeda,[§] Yang Luan,[†] Xin-Ming Qi,[†] Yuichi Sugiyama,[§] and Jin Ren*[,†]

[†]State Key Laboratory of Drug Research, Shanghai Institute of Materia Medica, Shanghai Institutes for Biological Sciences, Shanghai, China

[§]Laboratory of Molecular Pharmacokinetics, Graduate School of Pharmaceutical Sciences, The University of Tokyo, Tokyo, Japan

Supporting Information

ABSTRACT: Ingestion of aristolochic acid (AA), especially its major constituent aristolochic acid I (AAI), results in severe kidney injury known as aristolochic acid nephropathy (AAN). Although hepatic cytochrome P450s metabolize AAI to reduce its kidney toxicity in mice, the mechanism by which AAI is uptaken by renal cells to induce renal toxicity is largely unknown. In this study, we found that organic anion transporters (OATs) 1 and 3, proteins known to transport drugs from the blood into the tubular epithelium, are responsible for the transportation of AAI into renal tubular cells and the subsequent nephrotoxicity. AAI uptake in HEK 293 cells stably transfected with human OAT1 or OAT3 was greatly increased compared to that in the control cells, and this uptake was dependent on the AAI concentration. Administration of probenecid, a well-known OAT inhibitor, to the mice reduced AAI renal accumulation and its urinary excretion and protected mice from AAI-induced acute tubular necrosis. Further, AAI renal accumulation and severe kidney lesions induced by AAl in *Oat1* and *Oat3* gene knockout mice all were markedly suppressed compared to those in the wild-type mice. Together, our results suggest that OAT1 and OAT3 have a critical role in AAl renal accumulation and toxicity. These transporters may serve as a potential therapeutic target against AAN.

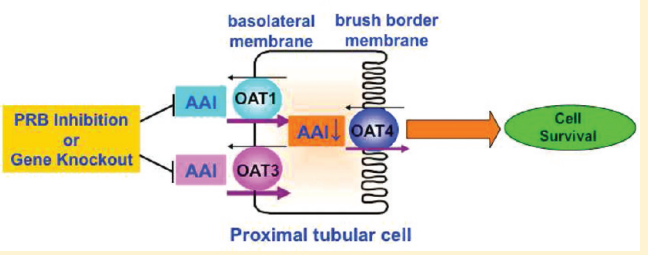

KEYWORDS: organic anion transporter, aristolochic acid nephropathy, kidney toxicity, *Oat1* and *3* knockout mice

INTRODUCTION

Aristolochic acid (AA) is a mixture of structurally related nitrophenanthrene carboxylic acids whose major nephrotoxic constituent is 8-methoxy-6-nitro-phenanthro[3,4-*d*]-1,3-dioxolo-5-carboxylic acid (AAI).[1] It is characterized as a carcinogen and nephrotoxin in many species including humans,[2] rabbits,[3] and rats.[4] AA has drawn extensive attention since the Belgian reported cases of nephropathy associated with the prolonged intake of Chinese herbal remedies containing AA, which were inadvertently included in slimming pills in the 1990s.[5,6] Although the sale of herbs containing AA has been prohibited worldwide since 2000,[7] they are still sold via the Internet.[8] The incidence of aristolochic acid nephropathy (AAN) is probably much higher than initially thought, especially in Asia and the Balkans.[9] Particularly in Asian countries such as China, Japan, and India where traditional medicines are very popular, the complexity of the herbal nomenclature system represents a high risk for AAN because of the frequent substitution of botanical products with AA-containing herbs.[10] In the Balkan regions, for instance, exposure to AA found in flour obtained from wheat contaminated with seeds of *Aristolochia clematitis* can be responsible for the so-called Balkan endemic nephropathy (BEN),[11] which shares many clinical and histological characteristics with AAN[12] and affects at least 25,000 inhabitants in certain rural areas of the Balkans.[13]

Previous studies have investigated the possible mechanisms for AAI-induced nephrotoxicity both *in vitro* and *in vivo*. AAI may directly cause acute renal toxicity and apoptosis through either the endoplasmic reticulum (ER) stress pathway or the mitochondrial cell death pathway in renal tubular cells.[14,15] Recently, the activation of the p53 pathway has been reported to participate in the process of apoptosis induced by AAI.[16] The levels of AAI have also been found to be about 3-fold higher in the kidney than in the liver 30 min after injection of 10 mg/kg AAI in mice, and it has been found that hepatic cytochrome P450s metabolize AAI and reduce its kidney toxicity.[17] However, the mechanism for kidney accumulation of AAI remains unknown.

Organic anion transporters (OATs) comprise a family of membrane transporters with multispecific substrates.[18] Over the past few years, various OATs, including OAT1,[19,20] OAT2,[21] OAT3,[22,23] and OAT4,[24] have been identified. Among them, OAT1 and OAT3 are the major OATs in the basolateral membrane of the proximal and distal tubules.[25−27] They are highly conserved across species, including humans, rats, and mice.[28] On

Received: December 4, 2010
Accepted: October 9, 2011
Revised: May 12, 2011
Published: October 10, 2011

one hand, these carriers protect the organism by secreting waste products, drugs, and other xenobiotics, including their metabolites. On the other hand, their activities can be associated with proximal tubular injury resulting from the accumulation of toxins. For example, ochratoxin A,[29] cephalosporins,[30] and indoxyl sulfate[31] have been shown to induce nephrotoxicity via OAT1- and OAT3-mediated uptake into the renal proximal tubules.

Recently, Bakhiya et al. demonstrated that AAI is an inhibitor of OAT1 and OAT3 and hypothesized that AA is a substrate based on inhibition and trans-stimulation data. Indeed, the hydrophobic part of a typical substrate for OAT1 has been reported to be of a certain size (4−10 Å), and the strength of the anionic charge is important to the interaction with OAT1.[18] In accordance with this, we measured that AAI possesses an anionic carboxyl group and a hydrophobic part about 7−8 Å. Therefore, in the present study we investigated whether OATs can mediate the transport of AAI and facilitate AAI induced nephrotoxicity under physiological conditions *in vivo* using OATs' pharmacological inhibitor probenecid (PRB) and Oat1 and Oat3 gene knockout (KO) mice, as well as directly detected the uptake of AAI by human embryonic kidney (HEK) 293 cells overexpressing human OAT1- and OAT3 (hOAT1- and hOAT3-HEK) at short exposure times and low concentrations *in vitro*. Here, we provide the first evidence that tubular OAT1 and OAT3 contribute to tubular uptake and renal accumulation of AAI *in vivo*. Inhibition or inactivation of these transporters plays a protective role in AAI-induced kidney-specific toxicity, which indicated a potential therapeutic target against AA-induced nephrotoxicity.

EXPERIMENTAL SECTION

Reagents. Probenecid (PRB), aristolochic acid I (AAI), *p*-aminohippurate (PAH), and estrone-3-sulfate (ES) were obtained from Sigma-Aldrich (St. Louis, MO, USA). The radiolabeled tracers [^{3}H]-PAH (specific activity 4.2 Ci/mmol) and [^{3}H]-ES (57 Ci/mmol) were purchased from Perkin-Elmer (Waltham, MA). Aristolactam I (ALI) was provided by Shanghai Chempartner Co. (Shanghai, China). Aristolochic acid Ia (AAIa) (purity 97%) was isolated from an *in vitro* metabolic activation system using microsomal mixtures as described previously.[32] The structure of AAIa was confirmed by NMR and mass spectrometry.

Cell Culture and Uptake Study. Mock, hOAT1-HEK, and hOAT3-HEK were established as described previously[33] and were grown in Dulbecco's modified Eagle's medium (Invitrogen, Scotland, U.K.) supplemented with 10% fetal bovine serum, penicillin (100 U/mL), streptomycin (100 μg/mL), and G418 sulfate (400 μg/mL) at 37 °C under 5% CO_2 atmosphere and 95% humidity. The cells were seeded into polylysine-coated plates (BD biosciences, Bedford, MA). The cell culture medium was replaced with 5 mM sodium butyrate 24 h before the transport study to induce the expression of OAT1 and OAT3.

The cells were seeded into 12-well tissue culture plates at a cell density of 2×10^5 cells/well 2 days before the start of the experiment. The cells were washed once with 0.5 mL of phosphate-buffered saline (PBS) and then incubated at 37 °C for 2 min in the presence of 0.6 mL of Krebs−Henseleit buffer (118 mM NaCl, 23.8 mM $NaHCO_3$, 4.83 mM KCl, 0.96 mM KH_2PO_4, 1.20 mM $MgSO_4$, 12.5 mM HEPES, 5 mM glucose, and 1.53 mM $CaCl_2$ at pH 7.4) containing 0.1 μM [^{3}H]-PAH or 0.1 μM [^{3}H]-ES adjusted with non-radiolabeled PAH or ES to indicate concentrations. At the end of the incubation, the medium was aspirated, and the cells were washed twice with 1 mL of ice-cold incubation buffer and lysed in 500 μL of 0.2 N NaOH. Aliquots (500 μL) were transferred into scintillation vials after adding 250 μL of 0.4 N HCl. The radioactivity associated with the cells and medium was determined by liquid scintillation counting after adding 3 mL of Clear-sol I (Nacalai Tesque, Kyoto, Japan). To determine the inhibitory effect of PRB, 0.1 μM [^{3}H]-PAH or 0.1 μM [^{3}H]-ES was adjusted with non-radiolabeled PAH or ES to 5 μM and incubated at 37 °C for 2 min with or without 1 mM PRB. For the AAI uptake study, hOAT1- and hOAT3-HEKs were seeded at a density of 2×10^5 cells/well in 6-well tissue culture plates. The cells were washed once with PBS and then incubated at 37 °C with Krebs−Henseleit buffer containing 10 μM AAI at 37 °C for various periods (0.5−10 min) or various concentrations of AAI (5−20 μM) at 37 °C for 0.5 min. After washing the cells thrice with PBS, the intracellular concentrations of AAI were determined using HPLC as described below. The protein content of the solubilized cells was determined using a BCA Protein Assay Kit (Pierce, Rockford, IL).

Animal Treatments. Male C57BL/6 mice (10−14 weeks old, 22−24 g) were obtained from the Shanghai Laboratory Animal Center. Male Oat1 KO and their corresponding WT mice (14−18 weeks old, 24−28 g) in a C57BL/6 background were kept at Charles River Laboratories International, Inc. (Yokohama, Japan), whereas male Oat3 KO and their corresponding WT mice (14−18 weeks old, 24−28 g) in a C57BL/6 background were kept at Oriental Yeast Co., Ltd. (Tokyo, Japan). All animal experiments were approved by the Animal Care and Use Committee of the Graduate School of Pharmaceutical Sciences, The University of Tokyo, and Shanghai Institute of Materia Medica, Chinese Academy of Sciences.

For the pharmacological inhibition study, C57BL/5 mice were treated as follows: (1) A single ip injection of AAI at 10 mg/kg or 20 mg/kg in isotonic saline was administered to the AAI group mice 30 min after administration of 10 mL/kg isotonic saline; these doses of AAI could induce most of the pathological characteristics of AAN including hypocellular interstitial fibrosis, tubular atrophy, limited interstitial infiltrates and relatively mild glomerular changes as we previously described.[34] Furthermore, according to the Chinese Pharmacopoeia 2000, normal human dose in clinical prescription for *Aristolochia manschuriensis* is 60 g/day/person; while the average content of AAI in it was reported to be 2610 μg/g,[35] the clinical exposure could be as high as 3.132 mg/kg/day (50 kg/person) when not considering the loss during the formulation preparation, so our doses are relevant to clinic. (2) The PRB + AAI group mice were ip injected with PRB at 150 mg/kg in 10 mL/kg isotonic saline, 30 min before the administration of AAI; this dosing regimen for PRB has been shown to inhibit organic anion transport.[36] The kidney, liver and serum levels of PRB at 15−120 min after AAI treatment in this experiment were determined to be 0.19−0.68 mM, 0.19−1 mM and 0.14−1.72 mM, respectively; the plasma protein unbound fraction of PRB is determined to be 0.77 ± 0.01 so the PRB concentration *in vivo* was high enough to inhibit the activity of OATs. (3) The PRB group mice were ip injected with PRB at 150 mg/kg 30 min before administration of 10 mL/kg isotonic saline. (4) The control group mice received two doses of isotonic saline at 10 mL/kg or 20 mL/kg.

For the gene knockout study, Oat1 and Oat3 KO mice were treated as follows: (1) mice from the WT and KO control groups received a single ip dose of isotonic saline at 20 mL/kg; and (2) mice from the WT and KO AAI groups received a single ip dose of AAI at 20 mg/kg in 20 mL/kg isotonic saline.

Serum Biochemistry and Histopathology Examinations. All the mice were sacrificed to collect blood, livers, and kidneys on day 7 after the last injection. Serum BUN and CRE were measured by an automatic HITACHI Clinical Analyzer model 7080 (Hitachi High-Technologies Corporation, Tokyo, Japan). The livers and kidneys were fixed in 10% formalin solution before embedding in paraffin for sectioning (3 μm thick). The sections were stained with hematoxylin and eosin (H&E) by a standard pathology procedure[37] and then evaluated by a pathologist.

Pharmacokinetics and Tissue Distribution Study. A single ip injection of PRB at 150 mg/kg or isotonic saline at 10 mL/kg was administered to C57BL/6 mice 30 min before a single ip injection of AAI at 10 mg/kg or 20 mg/kg. Blood samples were collected by tail bleeding with heparin-coated capillaries at various time points, and tissue samples were collected at 15, 30, 60, and 120 min after AAI injection. The blood samples (30 μL each) were mixed with an equal volume of isotonic saline and spun at 4000*g* for 5 min at 4 °C to separate the serum. The sera were then mixed with three volumes of methanol and spun again at 14000*g* for 5 min to remove precipitated proteins. Aliquots of the final supernates were analyzed and quantified for the levels of AAI and the metabolites AAIa and ALI by HPLC as described below.

Biliary and Urinary Excretion Experiments. The mice were anesthetized with ip injections of 50 mg/kg sodium pentobarbital. After abdominal dissection, the gallbladder was ligated, and the bile duct was cannulated with a polyethylene tube (UT-3; Unique Medical, Tokyo, Japan) to collect bile. The urinary bladder was cannulated with two polyethylene tubes (PE-50; Becton Dickinson, NJ). One cannula was fitted with a syringe filled with isotonic saline to wash the inside of the bladder, and the other cannula was used for the collection of urine and wash solution. Then the mice received a bolus administration of AAI at 10 mg/kg via the jugular vein with or without 150 mg/kg PRB pretreatment. Blood samples were collected from the opposite jugular vein at 1, 15, 30, 45, and 60 min. Bile and urine samples were collected in 30 min intervals into preweighed 0.6 mL microcentrifuge tubes. After every urine collection, the bladder was flushed with about 100 μL of isotonic saline, and the wash solution was added to the urine. The volumes of bile and urine samples were determined gravimetrically, with 1.0 as the specific gravity. Immediately after the last blood, bile, and urine sampling, the mice were sacrificed, and the liver and kidney were removed. The tissues were weighed and stored at −80 °C until quantification. Portions of the liver and kidney were added to one volume of isotonic saline (w/v) and homogenized. The plasma (25 μL), bile (10 μL), urine (10 μL), and tissue homogenates (100 μL) were deproteinized with 3 volumes of methanol (w/v), followed by centrifugation at 4 °C and 10000*g* for 10 min. Aliquots of the final supernates were analyzed and quantified for the levels of AAI and the metabolites AAIa and ALI by HPLC as described below.

Determination of AAI and Its Metabolites by HPLC. The quantification of AAI and its metabolites in the samples was performed on a HPLC system that consisted of a Waters 2695 separation module and a 996 photodiode-array (PDA) detector (Waters Associates, Milford, MA) using a Welchrom XB-C18 column (5 μm, 4.6 × 250 mm; Welch Materials, MD). An isocratic mobile phase of methanol:0.1% acetic acid in H_2O (7:3) at a flow rate of 0.8 mL/min was used for separation. The absorption spectra of AAI and its metabolites were recorded from 200 to 400 nm with the in-line PDA detector, and the chromatograms were acquired at 317 nm. LC−MS/MS analysis was also conducted on an Agilent 6300 LC/MSD Trap XCT Ultra (Agilent Technologies Deutschland GmbH, Waldbronn, Germany) to confirm and characterize AAI and its metabolites. The detection conditions referred to Xiao et al.[17]

Pharmacokinetic Analysis. The AUC(0−60min) for AAI and its metabolites was calculated by the trapezoidal rule. $X_{bile}(0-60min)$, which was calculated from the following equation, is the cumulative amount excreted into bile over 0 to 60 min:

$$X_{bile}(0-60min) = [C_{bile}(0-30min)V_{bile}(0-30min) + C_{bile}(30-60min)V_{bile}(30-60min)]/\text{body weight} \quad (1)$$

where C_{bile} is the compound concentration in the bile and V_{bile} is the total bile volume in 30 min.

$CL_{bile,p}$ was calculated from the following equation:

$$CL_{bile,p} = X_{bile}(0-60min)/AUC(0-60min) \quad (2)$$

$X_{liver}(60min)$ is the hepatic concentration at 60 min, with dimensions of milligrams per gram of liver.

$X_{urine}(0-60min)$, which was calculated from the following equation, is the cumulative amount excreted into urine over 0 to 60 min:

$$X_{urine}(0-60min) = [C_{urine}(0-30min)V_{urine}(0-30min) + C_{urine}(30-60min)V_{urine}(30-60min)]/\text{bodyweight} \quad (3)$$

where C_{urine} is the compound concentration in the bile and V_{urine} is the total bile volume in 30 min.

$CL_{urine,p}$ was calculated from the following equation:

$$CL_{urine,p} = X_{urine}(0-60min)/AUC(0-60min) \quad (4)$$

$X_{kidney}(60min)$ is the renal concentration at 60 min, with dimensions of milligrams per gram of kidney.

The plasma protein binding was determined by ultrafiltration using the disposable Microcon YM-30 device (Millipore Corporation, Bedford, MA, USA) as described previously.[38]

Statistical Analysis. All data are expressed as mean ± SD and were analyzed with Student's *t* test or the one-way analysis of variance followed by Newman−Keuls comparisons; $p < 0.05$ was considered as significant.

RESULTS

Both OAT1 and OAT3 Mediated the Transport of AAI. To determine whether AAI is transported by OATs, we examined intracellular AAI levels in hOAT1- and hOAT3-HEK cells. The uptake of prototypic substrates [^{3}H]-*p*-aminohippurate (PAH) by hOAT1-HEK and [^{3}H]-estrone-3-sulfate (ES) by hOAT3-HEK was dependent on their concentration (Figure 1A,B) and can be inhibited by probenecid (PRB), a well-known OAT inhibitor (Figure 1C,D). These results suggest that the uptake activities of OAT1 and OAT3 in these cells were ascertained. Higher intracellular AAI levels were observed in hOAT1- and hOAT3-HEK cells than in mock cells after incubation with 10 μM AAI for 0.5−2 min (Figure 1E) or 5−10 μM AAI for 0.5 min (Figure 1F). In addition, the uptake clearance of AAI (5−20 μM) was calculated in hOAT1- and hOAT3-HEK at 0.5 min. Both hOAT1- (Figure 1G) and hOAT3-HEK (Figure 1H) showed saturable uptakes of AAI. These results indicate that AAI is a substrate of OAT1 and OAT3.

PRB Inhibited the Renal Accumulation of AAI. To demonstrate that OATs are involved in the renal accumulation of AAI

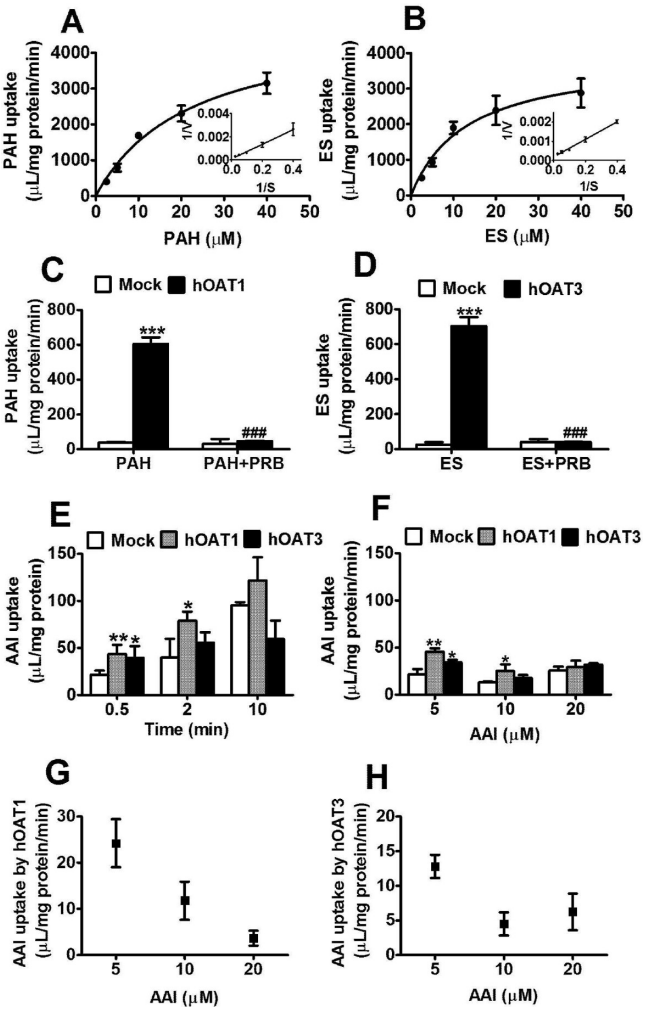

Figure 1. Time- and concentration-dependent uptake of AAI in hOAT1- and hOAT3-HEK. (A, B) Concentration-dependent (2.5−40 μM) uptake of PAH in hOAT1-HEK (A) and ES in hOAT3-HEK (B) is shown. (C, D) Inhibition study of the uptake of 5 μM PAH in hOAT1-HEK (C) and 5 μM ES in hOAT3-HEK (D) for 2 min in the absence or presence of 1 mM PRB is shown. (E−H) AAI uptake study. Mock, hOAT1-HEK and hOAT3-HEK were exposed to 10 μM AAI for 0.5−10 min (E) or 5−20 μM AAI for 0.5 min (F), after cells were washed and lysed, the intracellular AAI levels were determined using HPLC. The uptake clearances of AAI in hOAT1- (G) and hOAT3-HEK (H) calculated from (F) are also shown. Values are means ± SD (n = 3); $^{*}P < 0.05$, $^{**}p < 0.01$, $^{***}p < 0.001$ versus Mock, $^{\#\#\#}p < 0.001$ versus PAH or ES uptake in the absence of PRB, t test.

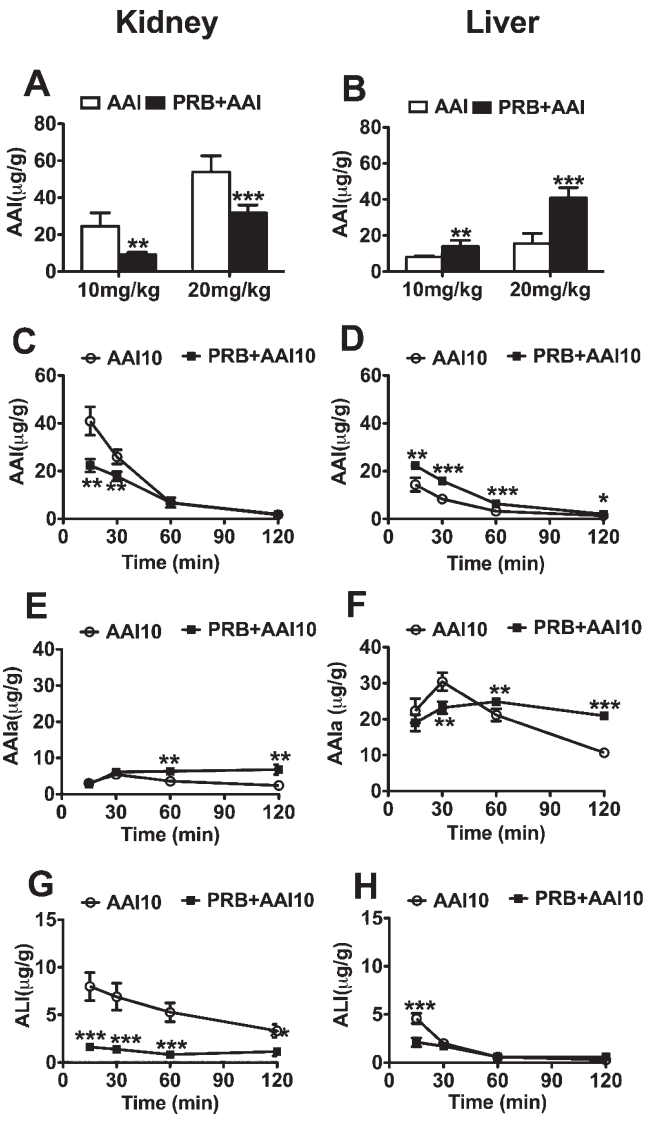

Figure 2. Effect of PRB on the hepatic and renal distribution of AAI and its metabolites. (A, B) Renal and hepatic levels of AAI at 30 min after an ip injection of AAI at 10 mg/kg or 20 mg/kg. (C−H) Time course of renal and hepatic levels of AAI (C, D), AAIa (E, F) and ALI (G, H) after an ip injection of AAI at 10 mg/kg. Values were mean ± SD (n = 5); $^{*}p < 0.05$, $^{**}p < 0.01$, $^{***}p < 0.001$ versus AAI group, t test.

in vivo, the tissue distributions of AAI and its metabolites were determined after intraperitoneal (ip) injection of AAI with or without PRB (Figure 2) in mice. PRB significantly decreased the renal accumulation of AAI 30 min after both 10 mg/kg and 20 mg/kg AAI injection (Figure 2A).

The levels of AAI in the liver were increased by PRB in both AAI doses (Figure 2B). Further, time-course study showed that PRB markedly reduced the renal levels of AAI until 60 min (Figure 2C), whereas it increased the hepatic levels of AAI until 120 min (Figure 2D). The renal levels of AAIa, a metabolite of AAI, were not influenced by PRB in 30 min, but were greatly increased from 60 min (Figure 2E). The hepatic levels of AAIa were slightly decreased at 30 min, but were markedly increased from 60 min (Figure 2F). The levels of aristolactam I (ALI), another metabolite of AAI, were remarkably decreased by PRB in the kidneys (Figure 2G), whereas the levels of ALI were greatly decreased in the liver at 15 min and slightly increased at 120 min (Figure 2H). These results indicate that OAT inhibition decreases tubular uptake and renal accumulation of AAI and its metabolites.

PRB Reduced the Serum Clearance of AAI. The serum AAI concentration was determined to further study the pharmacokinetics profile of AAI in the presence or absence of PRB in mice (Figure 3). PRB markedly increased the serum levels of AAI from 30 to 120 min after injection of 10 mg/kg AAI (Figure 3A) or from 30 to 180 min after injection of 20 mg/kg (Figure 3B). The calculated pharmacokinetic parameters, including maximum serum concentration (C_{max}) and area under the concentration−time curve (AUC) of AAI, were increased, whereas the apparent total body clearance (CL/F) of AAI was decreased by PRB

(Table 1). Similarly, the serum levels of AAIa, the only detectable metabolite of AAI in the serum, were also increased by PRB from 40 to 180 min after AAI injection at 10 mg/kg (Figure 3C) or 20 mg/kg (Figure 3D). The C_{max}, time of maximum serum concentration (T_{max}), AUC, and elimination half-life ($T_{1/2}$) of AAIa were increased, whereas the CL/F of AAIa was decreased by PRB (Table1). These results indicate that PRB reduces the serum clearance of both AAI and its metabolites.

PRB Reduced the Urinary Clearance of AAI but Increased Its Biliary Clearance. To elucidate how AAI was eliminated from the body after OAT inhibition reduced its renal accumulation, we determined its urinary and biliary clearances in the presence or absence of PRB *in vivo* (Figure 4). The urinary excretions of AAI and AAIa were greatly reduced by PRB (Figure 4A,C), whereas ALI cannot be detected in urine even after bolus injection of AAI at 10 mg/kg via the jugular vein. In contrast, the biliary excretions of AAI, AAIa, and ALI were substantially increased by PRB (Figure 4B,D,E). The pharmacokinetic parameters were summarized in Table 2. No significant difference was found in the AUC of AAI in the presence and absence of PRB. However, the AUC of AAIa was markedly increased. The cumulative amount excreted into urine over 0 to 60 min [$X_{urine}(0-60min)$] and the urinary clearance with regard to plasma concentration ($CL_{urine,p}$) of AAI and AAIa were all reduced. In comparison, the cumulative amount excreted into the bile over 0 to 60 min [$X_{bile}(0-60min)$] and the biliary clearance with regard to plasma concentration ($CL_{bile,p}$) of AAI and AAIa were increased. These results indicate that PRB reduces the excretion of both AAI and its metabolites into the urine, but increases their hepatobiliary excretion.

OAT Inhibition Protected Mice from AAI-Induced Nephropathy. To further characterize the possible role of OAT-mediated AAI transport *in vivo*, the effects of OAT inhibition on AAI-induced nephrotoxicity were investigated in C57BL/6 mice (Figure 5). The body weights of the mice were dose-dependently

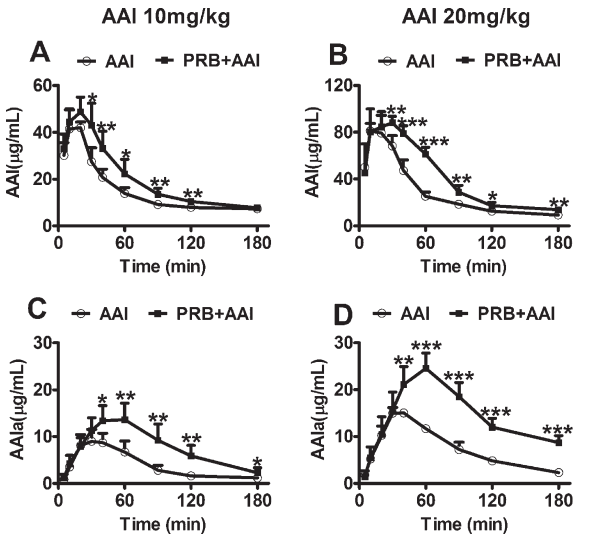

Figure 3. Serum levels of AAI and its major metabolite in AAI-treated and PRB+AAI-treated mice. Serum levels of AAI (A, B) and AAIa (C, D) after an ip injection of AAI at 10 mg/kg or 20 mg/kg. Values were mean ± SD (n = 5); *p < 0.05, **p < 0.01, ***p < 0.001 versus AAI group, t test.

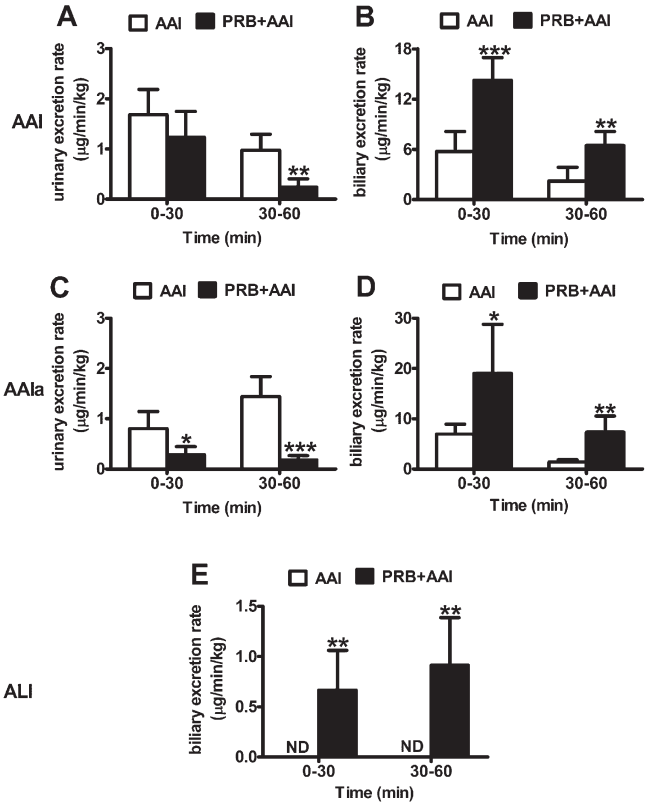

Figure 4. Effect of PRB on the urinary and biliary excretions of AAI and its metabolites. Urinary and biliary excretions of AAI (A, B), AAIa (C, D) and ALI (E) after an iv bolus injection of AAI at 10 mg/kg with or without PRB 150 mg/kg pretreatment at 30 min before. Values are mean ± SD (n = 5); *p < 0.05, **p < 0.01, ***p < 0.001 versus AAI group, t test.

Table 1. Pharmacokinetic Parameters for AAI and Its Major Metabolite AAIa in Mice from the PRB + AAI and AAI Treated Mice[a]

group	C_{max} (μg/mL)	T_{max} (min)	AUC (mg/mL·min)	$T_{1/2}$ (min)	CL/F (mL/min/kg)
AAI					
AAI10	44.3 ± 3.4	14.0 ± 5.5	3.11 ± 0.13	59.5 ± 1.0	3.22 ± 0.14
PRB + AAI10	51.8 ± 4.6*	18.0 ± 4.5	4.05 ± 0.52**	57.8 ± 5.3	2.50 ± 0.32**
AAI20	81.9 ± 6.5	16.0 ± 5.5	5.51 ± 0.57	49.7 ± 1.9	3.66 ± 0.36
PRB + AAI20	94.0 ± 9.1*	32.5 ± 5.0**	8.01 ± 0.53***	50.5 ± 4.1	2.51 ± 0.16***
AAIa					
AAI10	10.5 ± 0.6	27.0 ± 12.0	0.52 ± 0.04	29.4 ± 2.1	19.2 ± 1.5
PRB + AAI10	16.2 ± 1.1***	48.0 ± 11.0*	1.69 ± 0.02***	46.1 ± 7.5***	5.91 ± 0.07***
AAI20	15.3 ± 1.0	28.0 ± 8.4	1.08 ± 0.13	38.3 ± 6.1	18.6 ± 2.1
PRB + AAI20	25.2 ± 2.1***	66.0 ± 13.4***	3.52 ± 0.41***	78.3 ± 9.3***	5.75 ± 0.68***

[a] Values are mean ± SD (n = 5); *p < 0.05; **p < 0.01; ***p < 0.001 versus AAI group at the same dose.

dx.doi.org/10.1021/mp100418u |*Mol. Pharmaceutics* 2011, 8, 2183–2192

Table 2. Pharmacokinetic Parameters of AAI and AAIa after Iv Administration of AAI (10 mg/kg) with or without PRB (150 mg/kg) in C57BL/6 Mice[a]

	AAI		AAIa	
param	AAI	PRB + AAI	AAI	PRB + AAI
AUC (0−60min) (mg·min/mL)	3.05 ± 0.22	3.48 ± 0.24	0.55 ± 0.04	0.98 ± 0.10**
X_{liver}(60min) (μg/g liver)	6.00 ± 0.31	8.30 ± 0.87*	12.22 ± 1.12	10.14 ± 0.39
X_{bile} (0−60min) (μg/kg)	239 ± 23	621 ± 48***	251 ± 26	792 ± 150**
$CL_{bile,p}$ (mL/min/kg)	0.08 ± 0.01	0.18 ± 0.02**	0.45 ± 0.03	0.80 ± 0.10*
X_{kidney}(60min) (μg/g kidney)	7.42 ± 0.79	3.05 ± 0.49**	3.11 ± 0.49	2.38 ± 0.18
X_{urine} (0−60min) (μg/kg)	79.8 ± 9.4	43.9 ± 9.2*	67.4 ± 4.9	13.9 ± 3.8***
$CL_{urine,p}$ (mL/min/kg)	0.02 ± 0.00	0.01 ± 0.00*	0.10 ± 0.00	0.01 ± 0.00***

[a] Values are mean ± SE (n = 5); *P < 0.05 versus AAI group; **p < 0.01, ***p < 0.001.

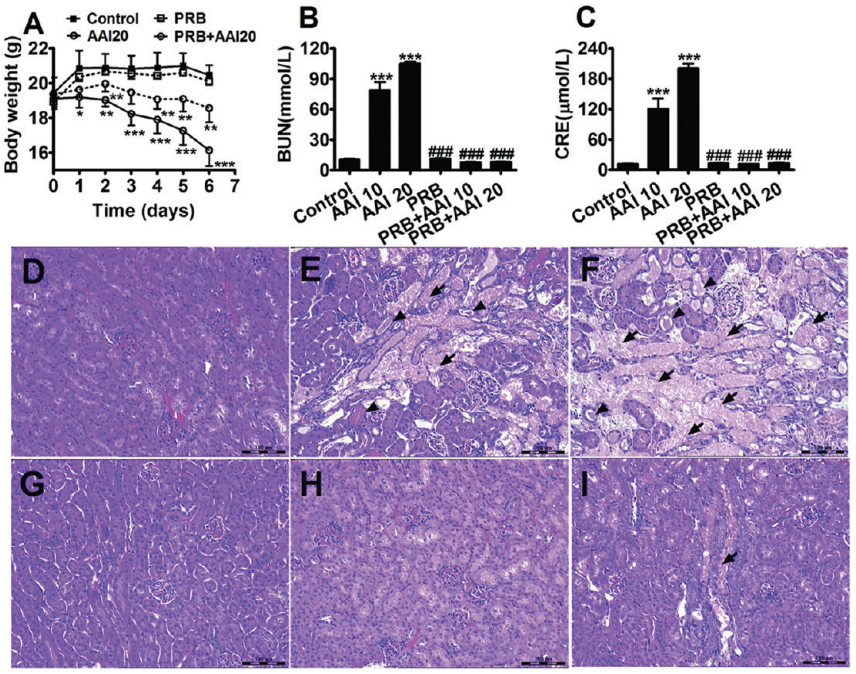

Figure 5. Effect of PRB on AAI-induced nephrotoxicity. (A) Body weight determined at the indicated time points after treatment. Data are mean ± SD (n = 5); *P < 0.05, **P < 0.01 versus control mice, two-way ANOVA analysis. (B, C) Serum biochemistry for kidney function: BUN (B); CRE (C). Values are mean ± SD (n = 5); ***p < 0.001 versus control group, ###p < 0.001 versus AAI group, one-way ANOVA analysis. Representative H&E staining of mouse renal cortex from indicated treatments, control (D), AAI 10 mg/kg (E), AAI 20 mg/kg (F), PRB (G), PRB + AAI 10 mg/kg (H) and PRB + AAI 20 mg/kg (I). Scale bar, 100 μm. Arrowheads, tubular cast; arrow, tubular necrosis.

reduced after injection of AAI. PRB inhibited this reduction (Figure 5A). PRB also markedly decreased the elevation of blood urea nitrogen (BUN) and creatinine (CRE) induced by AAI treatment (Figure 5B,C). Histologically, severe kidney lesions, including tubular necrosis, hyaline casts, and tubular dilation, were observed in the mice from the AAI group (Figure 5E,F), whereas these injuries were strikingly alleviated by PRB (Figure 5H,I). Furthermore, betamipron (BMP), another OAT inhibitor,[39] also protected mice from AAI-induced nephrotoxicity as evidenced by kidney function and histopathologic examinations (Figure S1 in the Supporting Information). These findings suggest that inhibition of OATs can protect mice from renal injury induced by AAI.

Both *Oat1* and *Oat3* Gene Knockout Protected Mice from AAI-Induced Nephropathy. To ascertain that the reduced nephrotoxic effects were indeed mediated by OATs, we compared the tissue distribution (Figure 6) and nephrotoxicity (Figures 7 and 8) of AAI in *Oat1* and *Oat3* KO mice with those of their wild type (WT) mice. After bolus injection of AAI at 10 mg/kg via the jugular vein (Figure 6), the renal concentrations of AAI in *Oat1* and *Oat3* KO mice were markedly reduced (Figure 6A,B), whereas there were no dramatic changes in the hepatic concentrations of AAI in *Oat1* or *Oat3* KO mice. There was no change in the tissue distribution of AAIa, whereas the renal concentration of ALI was greatly decreased in both *Oat1* and *Oat3* KO mice. The serum concentrations of AAI in *Oat1* and *Oat3* KO mice were not different from those in their WT mice counterparts after AAI injection (Figure S2 in the Supporting Information). These findings indicate that both *Oat1* and *Oat3* are responsible for the tubular accumulation of AAI.

Furthermore, the renal lesions in *Oat1* and *Oat3* KO mice were less severe than those in their WT mice after AAI injection.

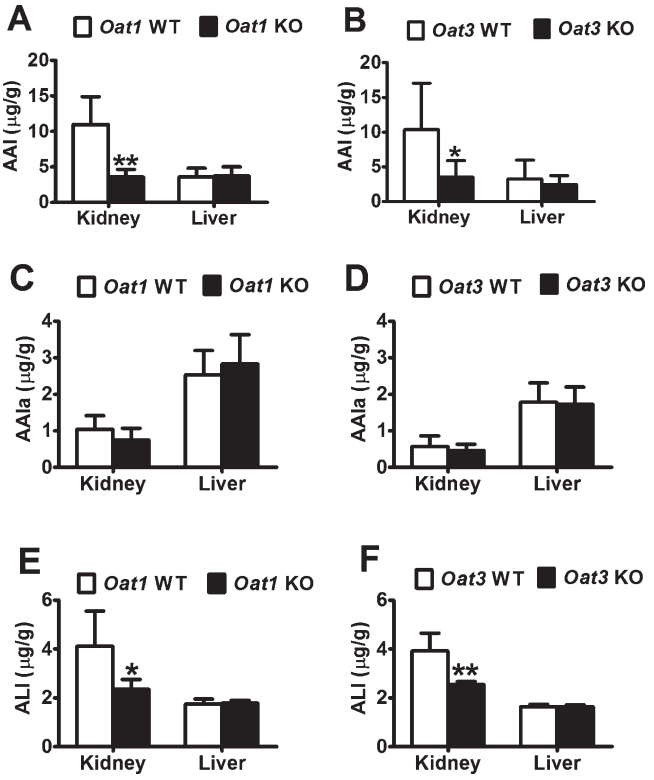

Figure 6. Effects of *Oat1* and *Oat3* gene knockout on the tissue distribution of AAI and its metabolites. Tissue levels of AAI (A, B), AAIa (C, D) and ALI (E, F) at 60 min after an iv bolus injection of AAI at 10 mg/kg in *Oat1* or *Oat3* KO mice. Values are mean ± SD (n = 4−6); $^{*}p < 0.05$, $^{**}p < 0.01$ versus WT group, t test.

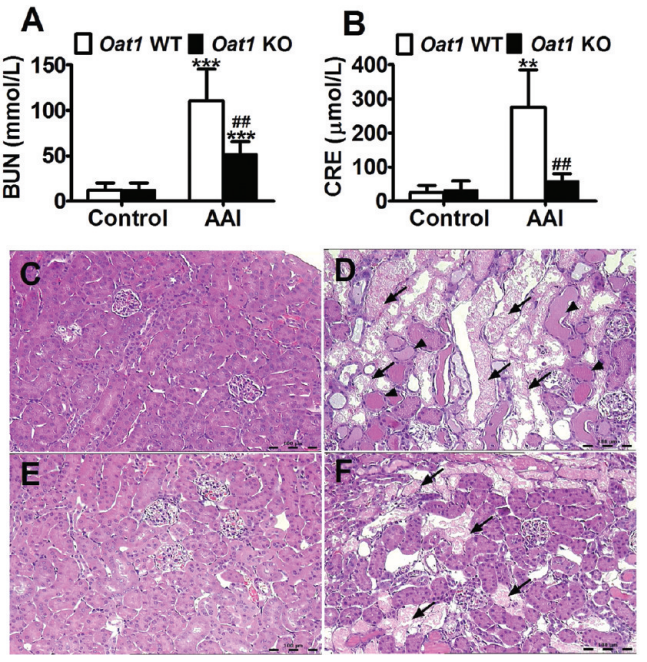

Figure 7. Effect of *Oat1* gene knockout on AAI induced nephrotoxicity. (A) BUN and (B) CRE from *Oat1* WT and KO mice, Values are mean ± SD (n = 3−6); $^{*}p < 0.05$, $^{**}p < 0.01$ versus control group, $^{\#}p < 0.05$ versus AAI group, one-way ANOVA analysis. (C−F) H&E staining of renal cortex: (C) *Oat1* WT control, (D) *Oat1* WT AAI 20 mg/kg, (E) *Oat1* KO control, (F) *Oat1* KO AAI 20 mg/kg. Results shown are representative microscope images for 3−5 mice in each group. Scale bar, 100 μm. Arrowheads, tubular cast; arrows, tubular necrosis.

In vehicle-treated groups, *Oat1* KO mice had similar serum BUN and CRE levels as WT mice. AAI treatment markedly increased the levels of BUN and CRE in WT mice, whereas AAI induced less increase of BUN and CRE in *Oat1* KO mice (Figure 7A,B). Accordingly, no obvious pathological abnormalities were observed in the kidneys of *Oat1* KO and WT mice in the vehicle-treated group (Figure 7C,E). AAI treatment caused less severe nephropathy (tubular necrosis, hyaline casts, and tubular dilation) in *Oat1* KO mice than in WT mice (Figure 7D,F; Table 3). Similarly, AAI-induced nephrotoxicity was less severe in *Oat3* KO mice than in WT mice, as evidenced by serum biochemistry (Figure 8A,B) and pathological examinations (Figure 8C−F; Table 3). In addition, three of the six *Oat1* WT mice and six of the thirteen *Oat3* WT mice died at day 7 after a single dose of 20 mg/kg AAI treatment, whereas all *Oat1* KO mice and *Oat3* KO mice survived (Table 3). These results indicate that both *Oat1* and *Oat3* gene knockout attenuated AAI-induced nephropathy in mice.

DISCUSSION

AA, especially the major constituent AAI, causes severe kidney lesions known as the AAN, but the molecular mechanisms for its kidney accumulation and toxicity remain unclear. In this study, we showed that the transport of AAI by OAT1 and OAT3 contributes to the nephrotoxicity of AAI. OAT1 and OAT3 were found to transport AAI in a concentration-dependent manner, and their deletion or inhibition can markedly reduce the renal levels of AAI, thus protecting mice from AAN.

In the renal tubules, membrane transport systems mediate the uptake and tubular secretion of endogenous and exogenous organic anions, including various drugs, toxins, and endogenous metabolites.[32] OAT1 and OAT3 are the main carriers that mediate the concentrative uptake of anionic compounds from the blood into renal proximal tubular cells, so the proximal tubule is the major site of renal injury.[28] Recently, Babu et al. found that treatment of the cells derived from the second portion of the proximal tubule (S_2) which stably express hOAT3 with AAI results in a significant reduction in viability compared with that of mock-treated cells rescued with the OAT inhibitor PRB.[40] Bakhiya et al. reported that OATs may be involved in the uptake of AAI into proximal tubular cells *in vitro*.[41] The levels of AAI−DNA adducts in hOAT1- and hOAT3-HEK were higher than that in mock cells, and these adducts were reduced by PRB. However, these experiments used a high concentration of AAI (100 μM) with a long exposure period (24 h) that might induce unspecific effects. In this study, we examined the uptake of AAI by hOAT1- and hOAT3-HEK under short exposure times and low concentrations of AAI *in vitro* to further detect the intrinsic transport activity of OAT1 and OAT3 under tracer conditions. AAI uptake in both hOAT1- and hOAT3-HEKs was greatly increased in an AAI concentration-dependent manner. We tried to further determine the binding affinity (K_m) of AAI to OAT1 and OAT3, but we could not detect the intracellular AAI when the concentration of AAI was lower than 5 μM under current HPLC or LC−MS/MS conditions and unfortunately we failed in the synthesis of ^{3}H labeled AAI. Also, no difference of the intracellular AAI levels was observed between hOAT1- or hOAT3-HEKs and Mock when the concentration of AAI was higher than

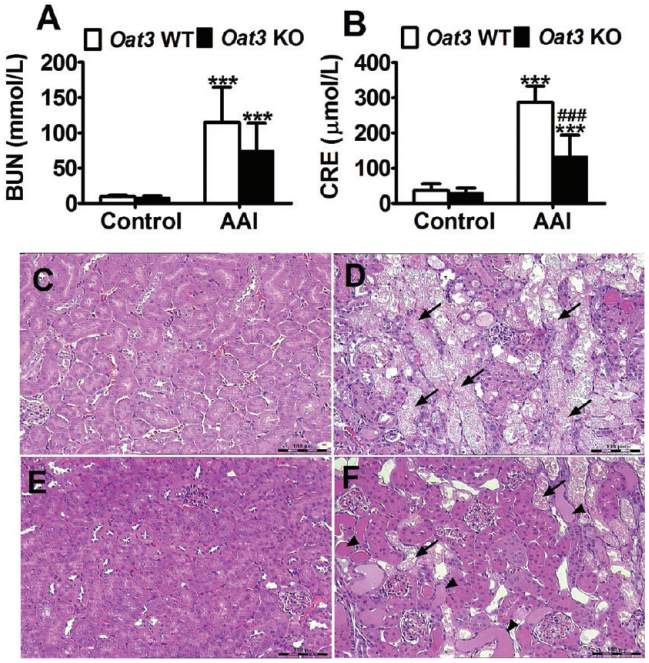

Figure 8. Effects of *Oat3* gene knockout on AAI induced nephrotoxicity. (A) BUN and (B) CRE from *Oat3* WT and KO mice. Values are mean ± SD ($n = 7$); $^{*}p < 0.05$, $^{***}p < 0.001$ versus control group, $^{###}p < 0.001$ versus AAI group, one-way ANOVA analysis. (C−F) H&E staining of renal cortex: (C) *Oat3* WT control, (D) *Oat3* WT AAI 20 mg/kg, (E) *Oat3* KO control, (F) *Oat3* KO AAI 20 mg/kg. Results shown are representative microscope images for 3−5 mice in each group. Scale bar, 100 μm. Arrowheads, tubular cast; arrows, tubular necrosis.

Table 3. Extent of Kidney Lesions in the KO and WT Mice Following AAI Dosing[a]

					no. of mice in each grade		
group	genotype	*N*	survival rate (%)	histology, *N*	+	++	+++
Oat1	WT	6	3 (50)	3	0	0	3
	KO	6	6 (100)	3	1	2	0
Oat3	WT	13	7 (53.8)	3	0	0	3
	KO	8	8 (100)	5	1	3	1

[a] The KO and WT mice (male, three-month-old) were treated with a single dose of 20 mg/kg AAI in saline by ip injection. Histopathology of tissues from each group was examined 7 days after treatment. The severity of lesions was graded as follows: +++, severe; ++, moderate; +, mild.

20 μM. So we expected that AAI bound to OAT1 and OAT3 with high affinities. Indeed, a potential binding mode between AAI and OAT1 (Figure S3 in the Supporting Information) predicted by molecular docking showed that AAI could bind to the binding site of OAT1 with a high affinity. Furthermore, AAI can inhibit the uptakes of a fluorescent substrate 6-carboxyl fluorescein by OAT1 and OAT3 with K_i values of 1.35 ± 0.31 μM and 0.71 ± 0.39 μM, respectively, while the K_i values for PRB were 34.74 ± 10.69 μM and 2.76 ± 0.87 μM, respectively (Figure S4 in the Supporting Information). Interestingly, when we were preparing this manuscript, one paper was published.[42] They used ^{3}H radiolabeled AA-I to evaluate the uptake of this compound in CHO cells expressing mOat1or 3 and found the K_m values were in the submicromolar range. These results indicate that AAI is a more potent inhibitor for OAT1 and OAT3 than PRB, as well as a high-affinity substrate for them as we expected.

As a well-known OAT inhibitor, PRB has been shown to decrease renal clearance, increase plasma concentration and protect against the nephrotoxicity of antiviral drugs (e.g., cidofovir) and β-lactam antibiotics (e.g., cephaloridine) by competing for their tubular secretion via OATs.[43,44] In this study, PRB was also found to decrease the renal distribution and urinary excretion of AAI and protect mice from AAI-induced nephropathy. Considering that AAI was less accumulated in the kidneys of *Oat1* and *Oat3* KO mice and that these mice were partially protected from AAN, OATs therefore play a crucial role in the tubular accumulation of AAI and induction of AAN.

Coadministration of PRB with methotrexate leads to increased serum half-life and delayed renal elimination for methotrexate, which is in turn associated with increased systemic toxicity.[45] In the present study, although PRB increased the systemic exposure and hepatic levels of AAI, no obvious hepatotoxicity or systemic toxicity occurred. This was indicated by the absence of changes in serum levels of alanine aminotransferase (ALT) and aspartate aminotransferase (AST), and histopathology (data not shown). This can be attributed to the extensive metabolism of AAI in the liver and excretion into the bile. BMP, another OAT inhibitor, also exerted similar protective effects against AAI-induced nephropathy without hepatotoxicity or systemic toxicity (Figure S1 in the Supporting Information, data not shown). Therefore, OAT inhibition can be a potential safe therapeutic pathway for AAN.

Given that AAI can be detected in the urine and bile, they can also possibly undergo efflux via some transporter(s) such as multidrug resistance-associated protein 2 (Mrp2), Mrp4, and Oat4 at the brush-border membranes in the kidney, as well as multidrug resistance 1, Mrp2, and breast cancer resistance protein at the canalicular membranes in the liver. Human OAT4, localized at the renal brush-border membrane, is involved in the transport of AAI.[42] Further studies are necessary to elucidate the efflux mechanisms of AAI *in vivo*. Interestingly, the $CL_{bile,p}$ values of AAI and AAIa were increased by the PRB treatment in this study. As expected, PRB inhibited the plasma protein (probably albumin) binding of these compounds, increased the plasma unbound fraction, and consequently increased the hepatic uptake and $CL_{bile,p}$. Indeed, increased hepatic levels of AAI were observed without influencing its plasma levels after bolus injection via the jugular vein. PRB also increased the plasma protein unbound fraction of AAI from 0.0006 ± 0.0002 to 0.0012 ± 0.0001 ($p = 0.0194$). Thus, a 2-fold difference in the biliary excretion clearance can be ascribed to the difference in plasma protein binding. Moreover, the inhibition of backflux from the cells to the blood, efflux from the cells to the bile, or intrahepatic metabolism by PRB may also be involved. The same mechanism may take place in the kidney; however, the significant inhibition of OAT-mediated renal uptake by PRB may have overcome the increase in plasma unbound fraction. A decrease in the renal distribution and $CL_{urine,p}$ was also observed.

In conclusion, our results suggest that both OAT1 and OAT3 are responsible for the basolateral uptake and accumulation of AAI in the kidneys, which are critical to the development of AAN. The clinical manipulation of the activities of OATs may represent a safe potential strategy for the prevention/treatment of this toxicant.

■ ASSOCIATED CONTENT

Supporting Information. Figures depicting effect of BMP treatment on AAI-induced nephrotoxicity, effects of *Oat1* and *Oat3* gene knockout on the serum levels of AAI and its metabolites, binding mode of compound AAI in OAT1, and effects of AAI and PRB on 6-carboxyl fluorescein uptake by hOAT1-HEK and hOAT3-HEK. This material is available free of charge via the Internet at http://pubs.acs.org.

■ AUTHOR INFORMATION

Corresponding Author

*Shanghai Institute of Materia Medica, 501 Haike Road, Zhangjiang Hi-Tech Park, Shanghai, China. Phone and fax: (86) 21-20231972. E-mail: jren@mail.shcnc.ac.cn.

Author Contributions

‡These authors contributed equally to this work.

■ ACKNOWLEDGMENT

We thank Yi-Zheng Wang for reading the manuscript, Fei Wang for molecular docking, Cheng-guo Feng for AAIa isolation, Wen-Sen Wu for histopathology evaluation, and Yuan-feng Wu, Guo-zhen Xing, Xiaofeng Xie, Jun Yao, Hiroyuki Kusuhara, Chun-yong Wu, Kentai Yoshida, Mari Miyajima, Ying Tian, Yan Li, Hua Sheng, Heng-Lei Lu, Bei-Yan Liu and Jing Lu for technical assistance. This work was supported by the National Basic Research Program (973 Program, 2006CB504701) and National Key Technologies R&D Program (No. 2009ZX09301-001, 2008ZX09305-007 and 2009ZX09501-033), and the Nagai Foundation Tokyo 2009 Doctoral Fellowship for International Researchers (to X.X.). Some of the work was reported at the XII International Congress of Toxicology and was summarized in the Conference Proceedings.

■ REFERENCES

(1) Shibutani, S.; Dong, H.; Suzuki, N.; Ueda, S.; Miller, F.; Grollman, A. P. Selective toxicity of aristolochic acids I and II. *Drug Metab. Dispos.* **2007**, *35*, 1217–1222.

(2) Nortier, J. L.; Martinez, M. C.; Schmeiser, H. H.; Arlt, V. M.; Bieler, C. A.; Petein, M.; Depierreux, M. F.; De Pauw, L.; Abramowicz, D.; Vereerstraeten, P.; Vanherweghem, J. L. Urothelial carcinoma associated with the use of a Chinese herb (Aristolochia fangchi). *N. Engl. J. Med.* **2000**, *342*, 1686–1692.

(3) Cosyns, J. P.; Dehoux, J. P.; Guiot, Y.; Goebbels, R. M.; Robert, A.; Bernard, A. M.; de Strihou, C. V. Chronic aristolochic acid toxicity in rabbits: A model of Chinese herbs nephropathy?. *Kidney Int.* **2001**, *59*, 2164–2173.

(4) Debelle, F. D.; Nortier, J. L.; De Prez, E. G.; Garbar, C. H.; Vienne, A. R.; Salmon, I. J.; Deschodt-Lanckman, M. M.; Vanherweghem, J. L. Aristolochic acids induce chronic renal failure with interstitial fibrosis in salt-depleted rats. *J. Am. Soc. Nephrol.* **2002**, *13*, 431–436.

(5) Vanherweghem, J. L.; Depierreux, M.; Tielemans, C.; Abramowicz, D.; Dratwa, M.; Jadoul, M.; Richard, C.; Vandervelde, D.; Verbeelen, D.; Vanhaelen-Fastre, R.; et al. Rapidly progressive interstitial renal fibrosis in young women: association with slimming regimen including Chinese herbs. *Lancet* **1993**, *341*, 387–391.

(6) Stiborova, M.; Frei, E.; Arlt, V. M.; Schmeiser, H. H. Metabolic activation of carcinogenic aristolochic acid, a risk factor for Balkan endemic nephropathy. *Mutat. Res.* **2008**, *658*, 55–67.

(7) Xue, X.; Xiao, Y.; Gong, L.; Guan, S.; Liu, Y.; Lu, H.; Qi, X.; Zhang, Y.; Li, Y.; Wu, X.; Ren, J. Comparative 28-day repeated oral toxicity of Longdan Xieganwan, Akebia trifoliate (Thunb.) koidz., Akebia quinata (Thunb.) Decne. and Caulis aristolochiae manshuriensis in mice. *J. Ethnopharmacol.* **2008**, *119*, 87–93.

(8) Gold, L. S.; Slone, T. H. Aristolochic acid, an herbal carcinogen, sold on the Web after FDA alert. *N. Engl. J. Med.* **2003**, *349*, 1576–1577.

(9) Debelle, F. D.; Vanherweghem, J. L.; Nortier, J. L. Aristolochic acid nephropathy: A worldwide problem. *Kidney Int.* **2008**, *74*, 158–169.

(10) Wu, K. M.; Farrelly, J. G.; Upton, R.; Chen, J. Complexities of the herbal nomenclature system in traditional Chinese medicine (TCM): Lessons learned from the misuse of Aristolochia-related species and the importance of the pharmaceutical name during botanical drug product development. *Phytomedicine* **2007**, *14*, 273–279.

(11) Grollman, A. P.; Shibutani, S.; Moriya, M.; Miller, F.; Wu, L.; Moll, U.; Suzuki, N.; Fernandes, A.; Rosenquist, T.; Medverec, Z.; Jakovina, K.; Brdar, B.; Slade, N.; Turesky, R. J.; Goodenough, A. K.; Rieger, R.; Vukelic, M.; Jelakovic, B. Aristolochic acid and the etiology of endemic (Balkan) nephropathy. *Proc. Natl. Acad. Sci. U.S.A.* **2007**, *104*, 12129–12134.

(12) de Jonge, H.; Vanrenterghem, Y. Aristolochic acid: the common culprit of Chinese herbs nephropathy and Balkan endemic nephropathy. *Nephrol., Dial., Transplant.* **2008**, *23*, 39–41.

(13) Arlt, V. M.; Stiborova, M.; vom Brocke, J.; Simoes, M. L.; Lord, G. M.; Nortier, J. L.; Hollstein, M.; Phillips, D. H.; Schmeiser, H. H. Aristolochic acid mutagenesis: molecular clues to the aetiology of Balkan endemic nephropathy-associated urothelial cancer. *Carcinogenesis* **2007**, *28*, 2253–2261.

(14) Qi, X.; Cai, Y.; Gong, L.; Liu, L.; Chen, F.; Xiao, Y.; Wu, X.; Li, Y.; Xue, X.; Ren, J. Role of mitochondrial permeability transition in human renal tubular epithelial cell death induced by aristolochic acid. *Toxicol. Appl. Pharmacol.* **2007**, *222*, 105–110.

(15) Hsin, Y. H.; Cheng, C. H.; Tzen, J. T.; Wu, M. J.; Shu, K. H.; Chen, H. C. Effect of aristolochic acid on intracellular calcium concentration and its links with apoptosis in renal tubular cells. *Apoptosis* **2006**, *11*, 2167–2177.

(16) Zhou, L.; Fu, P.; Huang, X. R.; Liu, F.; Lai, K. N.; Lan, H. Y. Activation of p53 promotes renal injury in acute aristolochic acid nephropathy. *J. Am. Soc. Nephrol.* **2010**, *21*, 31–41.

(17) Xiao, Y.; Ge, M.; Xue, X.; Wang, C.; Wang, H.; Wu, X.; Li, L.; Liu, L.; Qi, X.; Zhang, Y.; Li, Y.; Luo, H.; Xie, T.; Gu, J.; Ren, J. Hepatic cytochrome P450s metabolize aristolochic acid and reduce its kidney toxicity. *Kidney Int.* **2008**, *73*, 1231–1239.

(18) Miyazaki, H.; Sekine, T.; Endou, H. The multispecific organic anion transporter family: properties and pharmacological significance. *Trends Pharmacol. Sci.* **2004**, *25*, 654–662.

(19) Sekine, T.; Watanabe, N.; Hosoyamada, M.; Kanai, Y.; Endou, H. Expression cloning and characterization of a novel multispecific organic anion transporter. *J. Biol. Chem.* **1997**, *272*, 18526–18529.

(20) Hosoyamada, M.; Sekine, T.; Kanai, Y.; Endou, H. Molecular cloning and functional expression of a multispecific organic anion transporter from human kidney. *Am. J. Physiol.* **1999**, *276*, F122–128.

(21) Sekine, T.; Cha, S. H.; Tsuda, M.; Apiwattanakul, N.; Nakajima, N.; Kanai, Y.; Endou, H. Identification of multispecific organic anion transporter 2 expressed predominantly in the liver. *FEBS Lett.* **1998**, *429*, 179–182.

(22) Kusuhara, H.; Sekine, T.; Utsunomiya-Tate, N.; Tsuda, M.; Kojima, R.; Cha, S. H.; Sugiyama, Y.; Kanai, Y.; Endou, H. Molecular cloning and characterization of a new multispecific organic anion transporter from rat brain. *J. Biol. Chem.* **1999**, *274*, 13675–13680.

(23) Cha, S. H.; Sekine, T.; Fukushima, J. I.; Kanai, Y.; Kobayashi, Y.; Goya, T.; Endou, H. Identification and characterization of human organic anion transporter 3 expressing predominantly in the kidney. *Mol. Pharmacol.* **2001**, *59*, 1277–1286.

(24) Cha, S. H.; Sekine, T.; Kusuhara, H.; Yu, E.; Kim, J. Y.; Kim, D. K.; Sugiyama, Y.; Kanai, Y.; Endou, H. Molecular cloning and characterization of multispecific organic anion transporter 4 expressed in the placenta. *J. Biol. Chem.* **2000**, *275*, 4507–4512.

(25) Tojo, A.; Sekine, T.; Nakajima, N.; Hosoyamada, M.; Kanai, Y.; Kimura, K.; Endou, H. Immunohistochemical localization of multispecific

renal organic anion transporter 1 in rat kidney. *J. Am. Soc. Nephrol.* **1999**, *10*, 464–471.

(26) Kojima, R.; Sekine, T.; Kawachi, M.; Cha, S. H.; Suzuki, Y.; Endou, H. Immunolocalization of multispecific organic anion transporters, OAT1, OAT2, and OAT3, in rat kidney. *J. Am. Soc. Nephrol.* **2002**, *13*, 848–857.

(27) Hasegawa, M.; Kusuhara, H.; Sugiyama, D.; Ito, K.; Ueda, S.; Endou, H.; Sugiyama, Y. Functional involvement of rat organic anion transporter 3 (rOat3; Slc22a8) in the renal uptake of organic anions. *J. Pharmacol. Exp. Ther.* **2002**, *300*, 746–753.

(28) Bakhiya, N.; Stephani, M.; Bahn, A.; Ugele, B.; Seidel, A.; Burckhardt, G.; Glatt, H. Uptake of chemically reactive, DNA-damaging sulfuric acid esters into renal cells by human organic anion transporters. *J. Am. Soc. Nephrol.* **2006**, *17*, 1414–1421.

(29) Tsuda, M.; Sekine, T.; Takeda, M.; Cha, S. H.; Kanai, Y.; Kimura, M.; Endou, H. Transport of ochratoxin A by renal multispecific organic anion transporter 1. *J. Pharmacol. Exp. Ther.* **1999**, *289*, 1301–1305.

(30) Takeda, M.; Babu, E.; Narikawa, S.; Endou, H. Interaction of human organic anion transporters with various cephalosporin antibiotics. *Eur. J. Pharmacol.* **2002**, *438*, 137–142.

(31) Enomoto, A.; Takeda, M.; Tojo, A.; Sekine, T.; Cha, S. H.; Khamdang, S.; Takayama, F.; Aoyama, I.; Nakamura, S.; Endou, H.; Niwa, T. Role of organic anion transporters in the tubular transport of indoxyl sulfate and the induction of its nephrotoxicity. *J. Am. Soc. Nephrol.* **2002**, *13*, 1711–1720.

(32) Xiao, Y.; Xue, X.; Wu, Y. F.; Xin, G. Z.; Qian, Y.; Xie, T. P.; Gong, L. K.; Ren, J. beta-Naphthoflavone protects mice from aristolochic acid-I-induced acute kidney injury in a CYP1A dependent mechanism. *Acta Pharmacol. Sin.* **2009**, *30*, 1559–1565.

(33) Deguchi, T.; Kusuhara, H.; Takadate, A.; Endou, H.; Otagiri, M.; Sugiyama, Y. Characterization of uremic toxin transport by organic anion transporters in the kidney. *Kidney Int.* **2004**, *65*, 162–174.

(34) Xue, X.; Xiao, Y.; Zhu, H. L.; Wang, H.; Liu, Y. Z.; Xie, T. P.; Ren, J. Induction of P450 1A by 3-methylcholanthrene protects mice from aristolochic acid-I-induced acute renal injury. *Nephrol. Dial. Transplant.* **2008**, *23*, 3074–3081.

(35) Sorenson, W. R.; Sullivan, D. Determination of aristolochic acid I in botanicals and dietary supplements potentially contaminated with aristolochic acid I using LC-UV with confirmation by LC/MS: Collaborative study. *J. AOAC Int.* **2007**, *90* (4), 925–933.

(36) Emeigh Hart, S. G.; Wyand, D. S.; Khairallah, E. A.; Cohen, S. D. Acetaminophen nephrotoxicity in the CD-1 mouse. II. Protection by probenecid and AT-125 without diminution of renal covalent binding. *Toxicol. Appl. Pharmacol.* **1996**, *136*, 161–169.

(37) Gu, J.; Cui, H.; Behr, M.; Zhang, L.; Zhang, Q. Y.; Yang, W.; Hinson, J. A.; Ding, X. In vivo mechanisms of tissue-selective drug toxicity: effects of liver-specific knockout of the NADPH-cytochrome P450 reductase gene on acetaminophen toxicity in kidney, lung, and nasal mucosa. *Mol. Pharmacol.* **2005**, *67*, 623–630.

(38) Guo, B.; Li, C.; Wang, G.; Chen, L. Rapid and direct measurement of free concentrations of highly protein-bound fluoxetine and its metabolite norfluoxetine in plasma. *Rapid Commun. Mass Spectrom.* **2006**, *20*, 39–47.

(39) Takeda, M.; Narikawa, S.; Hosoyamada, M.; Cha, S. H.; Sekine, T.; Endou, H. Characterization of organic anion transport inhibitors using cells stably expressing human organic anion transporters. *Eur. J. Pharmacol.* **2001**, *419*, 113–120.

(40) Babu, E.; Takeda, M.; Nishida, R.; Noshiro-Kofuji, R.; Yoshida, M.; Ueda, S.; Fukutomi, T.; Anzai, N.; Endou, H. Interactions of human organic anion transporters with aristolochic acids. *J. Pharmacol. Sci.* **2010**, *113*, 192–196.

(41) Bakhiya, N.; Arlt, V. M.; Bahn, A.; Burckhardt, G.; Phillips, D. H.; Glatt, H. Molecular evidence for an involvement of organic anion transporters (OATs) in aristolochic acid nephropathy. *Toxicology* **2009**, *264*, 74–79.

(42) Dickman, K. G.; Sweet, D. H.; Bonala, R.; Ray, T.; Wu, A. Physiological and Molecular Characterization of Aristolochic Acid Transport by the Kidney. *J. Pharmacol. Exp. Ther.* **2011**, *338* (2), 588–597.

(43) Lacy, S. A.; Hitchcock, M. J.; Lee, W. A.; Tellier, P.; Cundy, K. C. Effect of oral probenecid coadministration on the chronic toxicity and pharmacokinetics of intravenous cidofovir in cynomolgus monkeys. *Toxicol. Sci.* **1998**, *44*, 97–106.

(44) Tune, B. M.; Wu, K. Y.; Kempson, R. L. Inhibition of transport and prevention of toxicity of cephaloridine in the kidney. Dose-responsiveness of the rabbit and the guinea pig to probenecid. *J. Pharmacol. Exp. Ther.* **1977**, *202*, 466–471.

(45) Aherne, G. W.; Piall, E.; Marks, V.; Mould, G.; White, W. F. Prolongation and enhancement of serum methotrexate concentrations by probenecid. *Br. Med. J.* **1978**, *1*, 1097–1099.